

# A Novel Front-hauling Architecture under Centralized Radio Access Network (C-RAN)

Haoran Mei, Mai Hassan, Limei Peng, and Pin-Han Ho

**Abstract**—Residential power line is considered a cost-effective communication media for building a digital indoor distributed network thanks to its ubiquity in the indoor environment. This paper investigates a front-hauling system under the split centralized radio access network (C-RAN) architecture, aiming to examine the feasibility of implementing common public radio interface (CPRI) over power line communication (PLC) channels. Particularly, we introduce a novel device called CPRI-PLC gateway (CPG) that provides a virtual CPRI link over the PLC channel to ensure high reliability and efficiency in delivering the CPRI hyper-frames (HFs) between the data unit (DU) and radio unit (RU). We examine the proposed CPRI over PLC system via extensive simulations in terms of the achievable throughput and reliability.

**Index Terms**—Centralized radio access network (C-RAN), common public radio interface (CPRI), front-haul, hybrid automatic repeat request (H-ARQ), impulsive noise detection & re-transmission (IND-Re), power line communication (PLC).

## I. INTRODUCTION

IN 5G communication systems, the user mobile data traffic is expected to reach more than seven-fold over the user data traffic in 2017, where the expected average mobile network data rate is 28.5 Mbps by 2022 [1]. [2] considers that deployment of low-power small base stations (BSs) is the most effective solution to meet this demand. This is particularly critical in the case of indoor service provisioning, in which the antennas should be located as close to the users as possible for line-of-sight (LOS) transmissions.

In [3], Huawei proposed the digital indoor distributed network (DIDN) as a promising indoor coverage solution in the evolution to 5G. The typical DIDN characteristics are met by the namely split C-RAN, which divides a conditional base station (BS) into three entities, i.e., central unit (CU), distributed unit (DU), and radio unit (RU) [4]. RUs, performing like active antennas, are distributed in each indoor chamber to

serve the indoor users, CUs are located at the central office to deal with the non-real-time base-band process, and DUs are placed between CUs and RUs to host the real-time baseband functionality. The high-speed CPRI links between RUs and DUs, and DUs and CUs, respectively, are called front-haul and mid-haul links.

Generally, optical fibers have been largely employed for the C-RAN front-haul links. Although with very low bit error rate (BER) and long reach, optical fibers may hardly be deployed in every corner of a building and cannot solely supply power to the end terminals. Note that installation of fiber optic based front-hauls for indoor services could be expensive if not impossible due to the requirement for infrastructural alteration. Alternatively, using PLC on in-building residential power lines could be a promising counterpart thanks to its ubiquity in the residential buildings and inherent electrical power supply that can greatly ease the deployment of the indoor devices [4], [5].

On the other hand, to take power lines as the media of C-RAN front-hauls, many issues arise due to the harsh nature of power lines. Note that the residential power lines are accessed by household appliances, such as PCs, refrigerators, cellphones, etc., and thus the PLC channel generally demonstrate a hostile environment that is subject to various noises. Specifically, the PLC channel is time-varying with Log-normal deep frequency dependent attenuation, which can hardly be described as additive white Gaussian noise (AWGN) and may directly impact the signal transmission [6]–[8].

According to their time-domain nature, the PLC noises can be classified into *background noise* and *impulsive noise* [9]. The impulsive noise is mainly caused by switching actions of rectifier diodes of electrical appliances [10], [11], and is considered the most harmful due to its significantly higher power spectral density (PSD) than the background noise. The spontaneous nature of the impulsive noise certainly causes a devastating corruption to the data transmitted over the power lines, and such corruptions can hardly be recovered by any coding mechanism. Thus, although mitigating the effect of the impulsive noise has been widely reported in the literature, they are not effective as most of these techniques focus on the handling, detection and removal of the data error caused by the impulses rather than to avoid the exposure of data to a noise impulse in the first place.

Note that impulsive noise mitigation has been extensively investigated under general OFDM systems, but to the best of our survey, has never been reported in the context of spread spectrum channels considered in the study [12]–[14]. In the event that we only follow the time-domain analysis, the state-of-the-art noise detection and removal techniques, such as

Manuscript received September 4, 2021; revised December 26, 2022; approved for publication by Jin-Ghoo Choi, Division II Editor, January 10, 2022.

The paper has been partly presented in the International Conference on Networking and Network Applications (NaNA) 2020.

This work was supported by the National Research Foundation of Korea (NRF) grant funded by the Korean Government (Grant No.: 2020R11A3072688) and National Science and Engineering Research Council (NSERC), Canada.

H. Mei and L. Peng are with the School of Computer Science and Engineering, Kyungpook National University, Daegu 41566, Republic of Korea, email: meihaoran, auroraplm@knu.ac.kr.

M. Hassan and P. H. Ho are with the Department of Electrical and Computer Engineering, University of Waterloo, ON, Canada, email: mai.hassan, p4ho@uwaterloo.ca.

L. Peng is the corresponding author.

Digital Object Identifier: 10.23919/JCN.2022.000003

Creative Commons Attribution-NonCommercial (CC BY-NC).

This is an Open Access article distributed under the terms of Creative Commons Attribution Non-Commercial License (<http://creativecommons.org/licenses/by-nc/3.0>) which permits unrestricted non-commercial use, distribution, and reproduction in any medium, provided that the original work is properly cited.

blanking/clipping, replacement, iterative threshold-based algorithms, time-frequency domain equalizers, and compressed sensing based techniques, strongly rely on signal processing at the receiver side [12], [14]. The main limitation for these techniques is that the noise characteristics must be known at the receiver, which is nonetheless not the case in the residential power lines. Thus, we have focused on re-transmission in the considered CPRI-PLC scenario.

This paper investigates using residential power lines as part of C-RAN front-hauls to support the transportation of time division multiplexed (TDM) CPRI frames for 5G indoor service provisioning, where a single-input single-output (SISO) PLC system is considered. Particularly, we introduce a novel device, namely CPRI-PLC-gateway (CPG), for enabling the power lines to support CPRI streams in the presence of the noisy PLC environment. Specifically, the CPG is installed at the DU and RU to form a CPG pair, which creates a virtual datapath that ensures the CPRI hyper-frames to be transported with satisfactory data rate and bit error rate (BER). This is achieved by the functional module of the proposed CPG, namely, impulsive noise detection & re-transmission (IND-Re) incorporated with Hybrid automatic repeat request (HARQ). We will show that the proposed approach can shape the power-lines into qualified CPRI links in supporting the desired indoor services.

The rest of this paper is organized as follows. We outline the in-door communication system in Section II.A, while studying PLC channel transfer function and noise models in Section II.B. Section III presents the IND-Re based HARQ scheme. We numerically analyze the simulation results in Section IV, and conclude this paper in Section V.

## II. SYSTEM MODEL

### A. System Architecture

Fig. 1 illustrates the split C-RAN scenario which has been proposed in [4], where a conventional BS is divided into three entities: CU, DU, and RU. The CU is located at the central office and connected to the DU via the first segment of front-haul(I)/mid-haul [15], mostly on an optical fiber link carrying the eCPRI or CPRI signal. The DUs are further connected to the RUs distributed in each indoor chamber via the second segment of the front-haul (II) carrying digital CPRI hyper-frames.

In this model, CPG serves as an agent to creating a virtual CPRI link between each DU and RU. Specifically, the CPG attached with the DU and RU are denoted as D-CPG and R-CPG respectively. To avoid any modification to the DU and RU, the CPG is made to be a plug-and-play device that can be deployed to interface between the front-haul system and the power lines, where a high-pass filter (HPF) is adopted at both CPGs to obtain the CPRI signals. Specifically, a 5-conductor three-phase line is deployed to connect the D-CPG and the indoor power distribution unit (PDU). The PDU is further connected to each R-CPG via one of the single phase lines containing 3 conductors: The phase/live (P), neutral (N) and protective earthing (PE) conductors. Finally, Each R-CPG

is connected to the corresponding apartment chamber via a distributed RU.

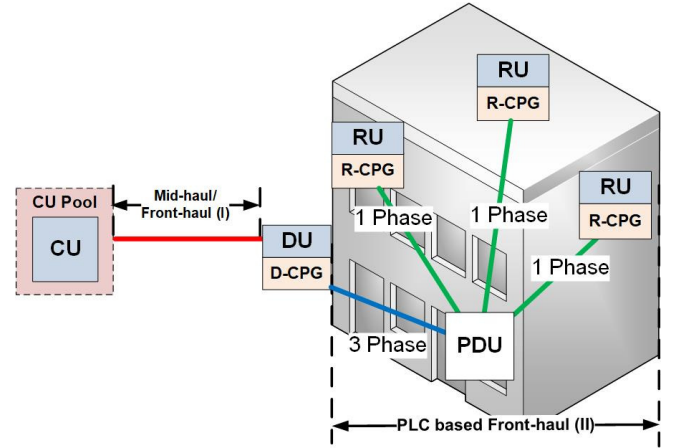


Fig. 1. Proposed split C-RAN system architecture for 5G indoor.

Fig. 2 illustrates the detailed functional diagram of the proposed PLC based front-hauling system. Here, the DU serves as a TDM hub that multiplexes/de-multiplexes the CPRI streams between the CU and the RUs. It may also bear some split functions from the original baseband unit (BBU); while how the splitting is performed is out of the scope of the study. The DU and RUs host CPRI modules without modification to ensure the communication using CPRI between them. The CPG contains the HARQ module that functions as the transmitter/receiver unit of selective repeat HARQ mechanism operating the re-transmission of HF, while the IND-Re modules execute the proposed re-transmission algorithm. The PDU, on the other hand, is a dummy device simply interfacing the three-phase line with the single-phase line. Each antenna of the RUs is connected to the PDU via one of the shared single-phase lines.

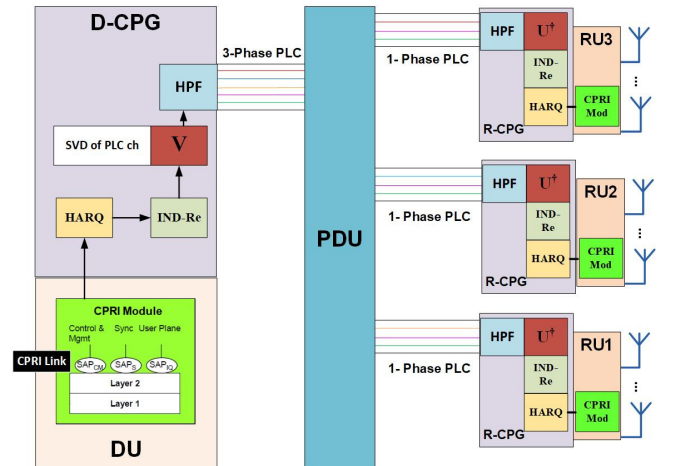


Fig. 2. The functional diagram of the proposed system architecture-DL.

Table I explains the specification of CPRI option 1, 2, and 3, i.e., length of basic frame and the corresponding CPRI requirement on the throughput. For CPRI-enabled PLC network, the protocol data unit is CPRI hyper-frame and its

size is varied from option to option but its duration is fixed as  $66.67 \mu\text{s}$  with the line rate which can be flexible according to the selected option.

TABLE I  
CPRI SPECIFICATION.

Option	Size of basic frame (bits)	Required data rate (Gbps)
1	128	0.6144
2	256	1.2288
3	512	2.4576

### B. PLC Channel Model

We consider the noise in the PLC as the sum of background noise and impulse noise. By assuming a balanced three-phase line with symmetrical components, the mutual coupling among the three main phase lines can be neglected [16]. Furthermore, the shunt admittance can be neglected as they contribute for  $< 5\%$  for power lines that are less than 80 km in length [17]. Therefore, the interference between the different single-phase lines can be neglected in comparison to the interference among the same single-phase line of different ports.

1) *Background noise model*: The background noise in PLC is a kind of colored Gaussian noise, which can be assumed to be cyclostationary with a level which strongly relies on the number and type of electrical devices connected to the network [11]. Such noise can be characterized in terms of PSD in unit of dBm/Hz through a simple model with three parameters [18] as follows:

$$S_{bg}(f) = a + b * |f|^c \quad [\text{dBm/Hz}] \quad (1)$$

where  $f$  is frequency in unit of MHz. The value of  $a$ ,  $b$ , and  $c$  have been specified by [9] as shown in the Table II and have been adopted in [19].

TABLE II  
BACKGROUND NOISE PARAMETERS USED.

	a	b	c
<b>Best case</b>	-140	38.75	-0.72
<b>Worst case</b>	-145	53.23	-0.337

2) *Impulsive noise model*: Possibly caused by switching transients in the network, impulsive noise could yield much higher PSD than that of background noise by 50 dB [20], causing destructive effect on the performance of PLC network. [20] also discovered that both width and inter-arrival time of an impulsive noise generally correspond to super-positions of several exponential distributions. The practical values of the impulse time width can be  $50\text{--}60 \mu\text{s}$  in the PLC while that of impulse inter-arrival time may reach  $0.015\text{--}0.02 \text{ ms}$ .

3) *Channel transfer function*: We represent the frequency response of PLC channel through a well-known top-down model adopted in [21] as follows

$$H(f) = A \sum_{i=1}^N |g_i(f)| e^{(a_0 + a_1 f^k) d_i} e^{-j2\pi f \tau_i}, \quad (2)$$

where  $A$ ,  $a_0$ ,  $a_1$ , and  $K$  are the variable attenuation parameters which have been specified in [22].  $N$  and  $g_i$  stand for the number of path and path gain respectively.  $f$  denotes the frequency while  $\tau$  means the delay of the path which can be given by

$$\tau = \frac{d_i}{v}, \quad (3)$$

where  $d_i$  and  $v$  are the path length and the velocity of propagation. In addition,  $v$  can be calculated from the speed of light  $c_0$  and the dielectric constant of the insulating material as

$$v = \frac{c_0}{\sqrt{\epsilon_r}}. \quad (4)$$

## III. PROPOSED FRONT-HAUL USING CPG

The proposed CPG is a device aiming to enable the power line to serve as the front-haul link while being completely transparent to the CPRI protocol operations between the DU and RU. The target of the CPG is to provide robust function for mitigating the malicious effect high BER and thus high frame error rate along the PLC channel via the HARQ based IND-Re mechanism.

### A. Impulsive Noise Detection & Re-transmission (IND-Re)

Since the impulsive noise is several folds stronger than the background noise with a time span of  $4\text{--}100 \mu\text{s}$ , it definitely damages one or two hyper-frames. Note that the bit errors can only be restored in the data plane that will cause considerable delay and additional processing overhead.

IND-Re is positioned to mitigate the malicious effect of impulsive noise by restoring the lost hyper-frames via a light-weight re-transmission upon the detection of any impulsive noise. Specifically, the proposed IND-Re has the transmitter and the receiver CPGs (i.e., D-CPG and R-CPG) to constantly sense the peak to average power ratio (PAPR), calculated as  $10 \log_{10}(P_s/P_{\text{mean}})$ , every one HF duration ( $\Delta t = 66.67 \mu\text{s}$ ). The impulsive noises can be detected when the sensed PAPR is greater than a certain threshold ( $Th = 10 \text{ dB}$  as the background-to-impulsive noise ratio is set to  $\Gamma = 0.1$ ), and the impulsive noise is passed when the sensed PAPR drops below another threshold.

Such an IND mechanism can greatly facilitate the efficiency of the HARQ protocol operation. When an impulsive noise is detected, the HARQ transmitter simply holds the transmission, while the receiver drops the currently received HF. The transmitter initiates re-transmission of the HF held due to the impulsive noise, while the receiver starts to take the next received HF as soon as impulsive noise is determined passed. With this, redundant re-transmissions can be avoided particularly when a HF is received with its acknowledgment (ACK) destroyed by the impulsive noise. Instead, the receiver will re-transmit the buffered ACKs and meanwhile accept the next incoming HF. While waiting for that ACK, the transmitter continues to send new HFs to maximize the channel utilization. After a pre-defined timeout, it initiates the re-transmission of the HFs if that ACK is not received and vice versa.

---

**Algorithm for impulsive noise detection/  
re-transmission (IND-Re)**


---

**Input:**  $\{P_{\text{mean}}\}, \{\Gamma\}$ 


---

1. Set  $Th = 10 \log_{10}(1/\Gamma)$ ,  $\Delta t = 66.67 \mu s$
  2. Measure  $P_s$
  3. While  $10 \log_{10}(P_s/P_{\text{mean}}) > Th$ , Loop
    - a. Transmitter: Hold hyper-frame transmission
    - b. Receiver: Discard incoming hyper-frame
    - c. Measure  $P_s$  over time =  $\Delta t$
  4. end
  5. Transmitter: Transmit CPRI hyper-frame
  6. Receiver: Accept incoming hyper-frame
- 

With HARQ, the receiver acknowledges each received CPRI HF in the vendor specific fields of the CPRI HF [23] in the reverse direction. The readily present frame check sequence (FCS) based on cyclic redundancy check (CRC) in the Control and Management (C&M) information of the CPRI hyper-frame is used for hyper-frame error checking [23].

#### IV. SIMULATION

The simulation is divided into two parts. One is with a  $3 \times 3$  single user (SU) MIMO PLC channel and the other is with an SISO PLC channel. The former stands for the case where a single phase line of all the three P, N and PE conductors are used to provision a single RU, while in the later case each of the connectors is used to connect with an RU.

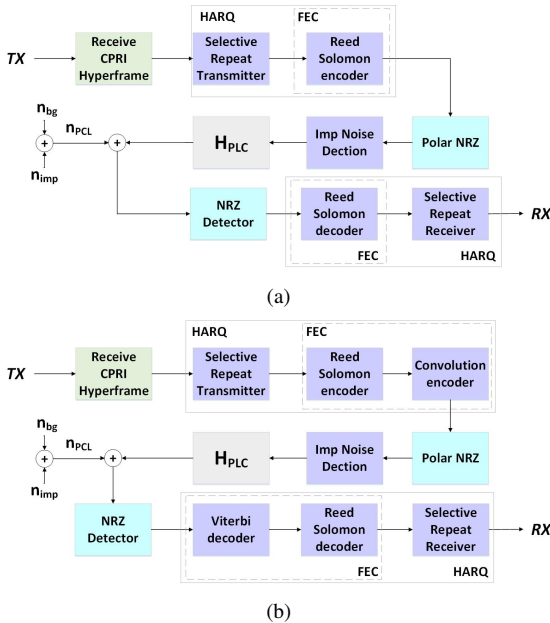


Fig. 3. Link level simulator block diagram: (a) Single code scenario and (b) concatenated code scenario.

We conduct a two-stage simulation, i.e., a link-level simulator (LLS) in the first stage for physical signal communications and a discrete event simulator (DES) in the second stage for the channel access of hyper-frames. Since the PLC channel

should be idle once the transmitter detects an impulsive noise in IND-Re, we do not consider impulsive noise in LLS and handle the impulsive noise in DES. The FEC function and IND-Re mechanism are implemented in both LLS and RES. Figs. 3(a) and 3(b) illustrate the block diagram LLS when using the single block coding scheme and the concatenated code scheme, respectively. In concatenated code scheme, the CC acts as an inner code to deal with random errors while the RS code serves as an outer code to correct burst errors caused by the Viterbi decoder and noise from channel.

TABLE III  
PARAMETERS FOR ERROR CORRECTION MECHANISM.

RS encoding	
(N, K)	(192,128) (224,128) (128, 64) (144, 64) (168, 64) (192, 64)
Convolution encoding	
Octal generator polynomial	[171, 133] [171, 133, 165]

Our simulation approach is given as follows. We first obtain the BER performance of PLC channels in LLS. The outcomes of the LLS are used in DES to simulate an integrated PLC system, including the SR-ARQ scheme and IND-Re. In the DES stage, we evaluate the system throughput efficiency, i.e.,  $\eta$ , and various delays. The throughput efficiency  $\eta$  determines whether the system capacity satisfies the CPRI requirement on throughput and is calculated by

$$\eta = \frac{\theta_{sys}}{\theta_{CPRI}}, \quad (5)$$

where  $\theta_{sys}$  refers to the system capacity in the simulation and  $\theta_{CPRI}$  is the CPRI specification on throughput for each option as shown in Table I. The impact of window size and error correction schemes on the system performance are also evaluated. Table III shows the configuration of error correction scheme applied in the simulation.

We consider the full-duplex bi-directional communication model by implementing the power lines in both directions. The interval rate of frames is equal to a CPRI HF duration. The occurrence rate and duration of an impulse noise are fixed as  $51.1 s^{-1}$  [20] and  $60 \mu s$  [24], respectively. This ensures that an impulsive noise can completely exhibit its negative effect on the system performance within a limited simulation time. The signal propagation velocity along the PLC channel is  $150 m/\mu s$ , which is calculated by (4) with the dielectric constant  $\epsilon_r$  of four in [25]. We also consider the worst background noise case in this experiment.

##### A. Front-haul on a $3 \times 3$ MIMO PLC Channel

Four scenarios are considered in this part of simulation:

**Sc1: CPRI Only:** Sending CPRI HFs without any modifications.

**Sc2: CPRI + HARQ:** CPRI HFs are sent over the power line with HARQ.

**Sc3: CPRI + IND-Re:** CPRI HFs are sent onto the power line while applying the proposed IND-Re.

**Sc4: CPRI+HARQ+IND-Re:** CPRI hyper-frames are sent onto the PLC line while enabling HARQ and IND-Re.

In all scenarios, polar non-return to zero (P-NRZ) is applied. The main evaluating metric for our system is the bit error rate (BER) and frame error rate (FER). In (6), the instantaneous capacity ( $C_{MIMO}$ ) of the PLC MIMO channel is calculated [26].

$$C_{MIMO} = \sum_{n=1}^{N_f} \Delta f \sum_{i=1}^{N_p} \log_2 \left( 1 + \frac{P_{T_x}(f_n) \lambda_i(f_n)}{N_{R_x}(f_n) N_p} \right) \quad (bps), \quad (6)$$

where  $\lambda_i(f_n)$  is the eigenvalues of  $HH^\dagger$  at a given frequency  $f_n$ .  $P_{T_x}(f_n)$  is the transmitted power and  $N_{R_x}(f_n)$  is the noise at the receiver.  $N_f$  is the number of samples in the frequency range,  $\Delta f$  is the sampling frequency used (frequency step) and  $N_p$  is the number of transmit/receive ports used [26].

The parameters used in the simulations are shown in Table IV. The regulations of general electro-magnetic compatibility (EMC) have been respected; such that the maximum PSD is set to  $-50$  dBm/Hz up to 30 MHz and to  $-80$  dBm/Hz for higher frequencies [27]. The system is simulated with bandwidth that extends to include the very high frequency band ( $\leq 300$  MHz). Moreover, to pursue a more conservative approach the maximum length (800 m) of a PLC system recorded in the literature has been used; despite the fact that within a full apartment building the length might not exceed 100 m.

TABLE IV  
SYSTEM SIMULATION PARAMETERS USING CPRI OPTION 1 FOR MIMO PLC FRONT-HAUL.

Parameters	Values
$E_b/N_0$ range	$-20$ – $50$ dB
Power line length	800 m
MIMO PLC ports (3-Phase)	6 Tx/Rx ports
PLC BW / port	1–300 MHz
Chip rate ( $\Delta f$ )	3.84 MHz
HARQ limit/frame ( $T$ )	4 re-transmission
RS-FEC rate	(134,128)
Interleaver rate	32
Selective repeat window	75 hyper frame
IND-Re threshold ( $Th$ )	10 dB
IND-Re mean power ( $P_{mean}$ )	$-115$ dB
CPRI hyper frame size	256 basic frames
CPRI hyper frame duration	66.67 $\mu s$
CPRI frame size	150 hyper-frames
CPRI frame duration	10 ms

Fig. 4 presents the system BER and Fig. 5 shows the FER for all the four scenarios. When the CPRI signal is sent over the PLC channel without any modifications, the BER and FER are extremely high even for high SNRs; therefore, its not possible to implement the system as such. HARQ improves the system performance with imposed limitation of 4 times on the number of HF re-transmissions. For SNR higher than 20 dB the residual bit error rate is recorded as zero with  $10^{13}$  simulated bits (i.e.,  $BER < 10^{-12}$ ).

Compared with bare CPRI, the use of IND-Re yields a clear positive impact on BER and FER. When IND-Re is applied, for SNR higher than 40 dB, the number of bits received in error

reaches zero without any re-transmission by higher layers. We have seen that zero residual BER and FER can be achieved for  $SNR > -15$  dB when both HARQ and IND-Re are used in the system simulations with  $10^{13}$  bits and 474 HF's simulated per SNR.

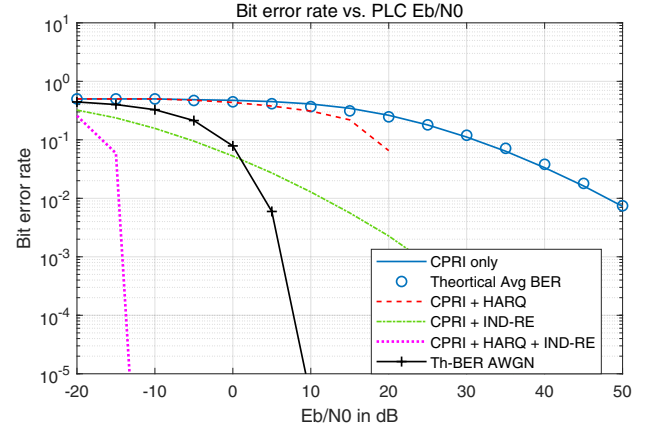


Fig. 4. Simulations BER outcomes.

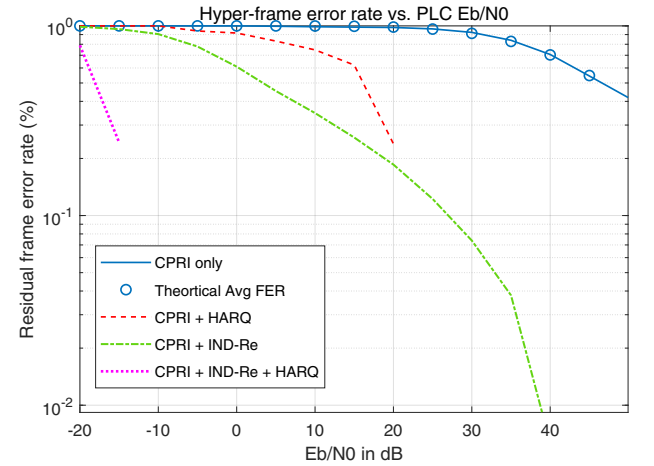


Fig. 5. Simulations FER outcomes.

Each of the four scenarios has been run 20 times per port, the mean and maximum capacity and effective throughput values at  $E_b/N_0 = 35$  dB are reported in Table V. Higher data rates can be achieved by expanding the bandwidth further in the very-high-frequency range ( $> 300$  MHz) [28]. The effective throughput when both HARQ and IND-Re are used constitutes for  $\sim 89\%$  of the system full capacity.

TABLE V  
EFFECTIVE THROUGHPUT OUTCOMES FOR  $E_b/N_0 = 35$  dB: MIMO PLC ( $6 \times 6$ ), SAME CIRCUIT, 10 RUNS.

Outcomes (Gbps)	Sc. 1	Sc. 2	Sc. 3	Sc. 4
Mean sys. cap.	5.465			
Max sys. cap.	12.72			
Mean thrpt.	0.83	0.6630	5.0977	4.9061
Max thrpt.	2.0405	1.544	11.8721	11.4260

### B. Front-haul on a SISO PLC Channel

This section evaluates the proposed PLC scheme on an SISO PLC channel through simulation experiments for CPRI options 1, 2, and 3 using parameters shown in Table VI. We consider CPRI option 3 when evaluating the impact of window size on throughput and use RS (192, 128) for FEC. Fig. 6 illustrate the throughput performance under SNRs for different window sizes, i.e., 4, 8, and 16. We consider a data rate of 5 Gbps, from the CPRI perspective. A larger window size indicates higher throughput efficiency under lower SNR, which is more obvious for larger data rate as shown in Fig. 6.

TABLE VI  
SYSTEM SIMULATION PARAMETERS FOR SISO PLC FRONT-HAUL.

Parameters	Values
E <sub>b</sub> /N <sub>0</sub> range	0–30 dB
Power line length	100 m
Propagation speed	150 m/μs
PLC bandwidth	1–300 MHz
Chip rate Δf	3.84 MHz
Selective repeat window	4–16 hyper frames
CPRI hyper frame size	256 basic frames
CPRI hyper frame duration	66.67 μs
Processing delay	10 μs
Data rate	5 Gbps

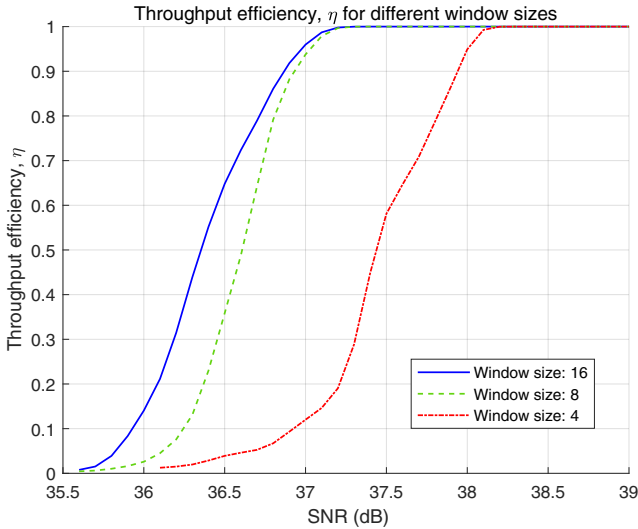


Fig. 6. Throughput under different window size with 5 Gbps data rate.

We evaluate the queuing and transmission delays for the successfully transmitted HF to investigate the impact of window size on the system delay, as shown in Figs. 7(a) and 7(b). Fig. 7(a) shows that the average queuing delay increases slightly with increasing window size.

Fig. 7(b) shows that extending the window size can significantly decrease the transmission delay. However, this impact decreases with the increasing SNR, i.e., from 36 dB to 36.5 dB and 40 dB, since the system capacity gradually reaches its upper bound. On the other hand, the average transmission delays are the same for all window sizes when SNR is large enough.

Then we simulate for CPRI options 1, 2, and 3 when the window size is 16.

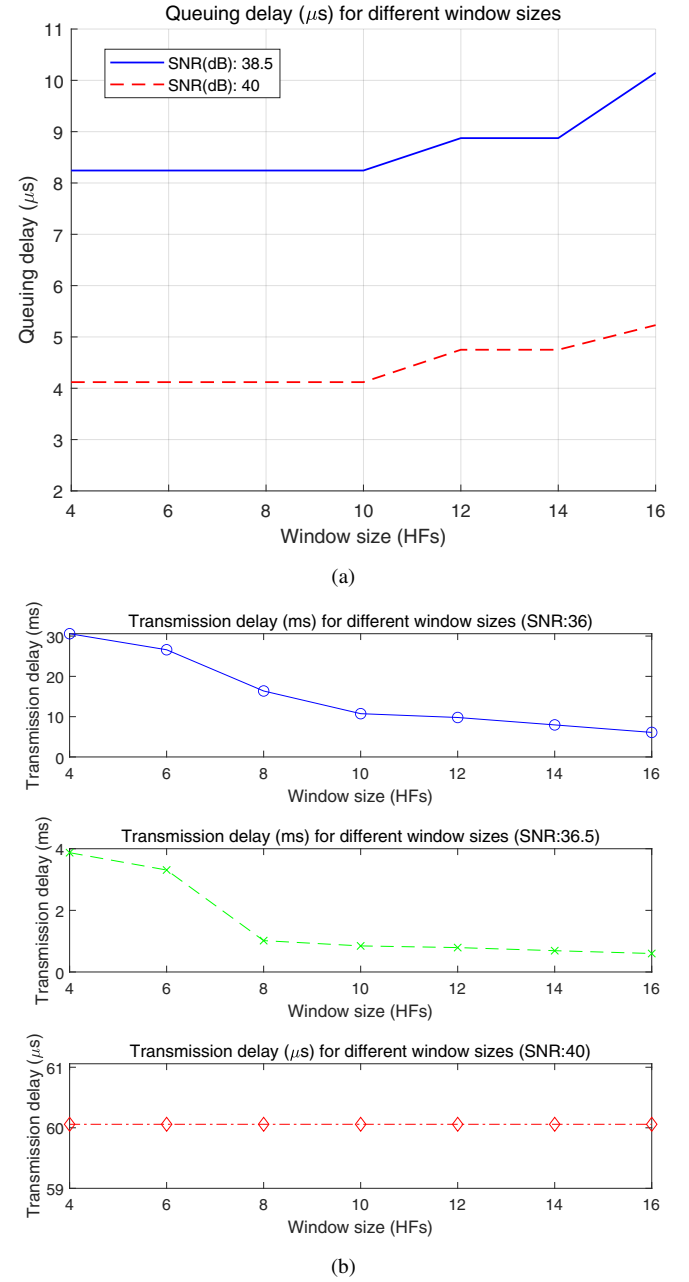


Fig. 7. System delay for Option 3 under different window size: (a) Average queuing delay and (b) average transmission delay.

Fig. 8 shows the minimum SNR (or maximum BER) required for the system to meet the CPRI specification for the three CPRI options. The higher option demands higher SNR to reach the needed throughput by CPRI, i.e.,  $\eta = 1$ , because hyper-frames with larger sizes demand lower BERs for successful transmission. Specifically from Fig. 8, the minimum SNR allowed for CPRI option 3 is close to 37 dB, which corresponds to a BER below  $10^{-4}$ . Therefore, it is critical to guarantee a BER lower than  $10^{-4}$  at low SNR when adopting CPRI option 3 for the CPRI link over PLC noisy channel.

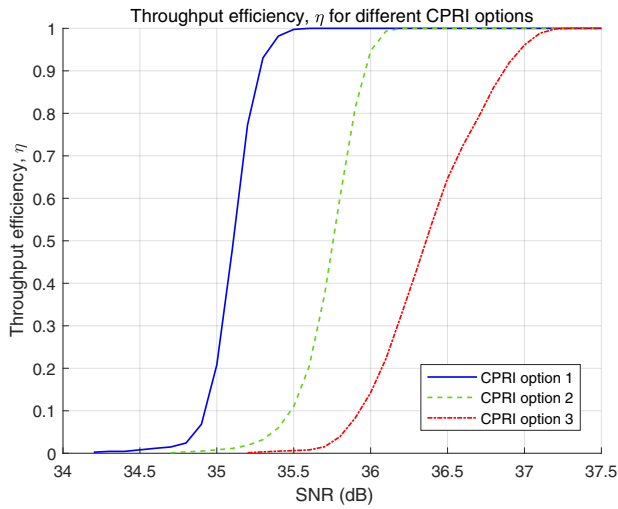
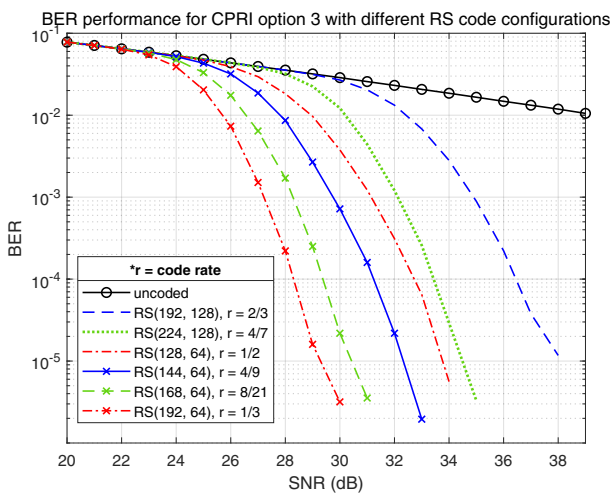
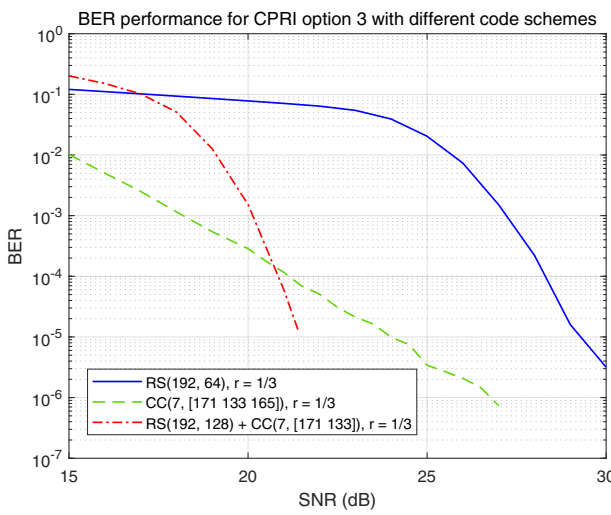


Fig. 8. Throughput efficiency for CPRI option 1, 2, and 3.



(a)



(b)

Fig. 9. BER performance for option 3 under different error correction configurations.

Modifying the FEC configurations is an appropriate way to reduce the minimum SNR needed to reach a specific BER value. For this, We compare the BER for RS with different code rates as error correction mechanisms for CPRI option 3 in the LLS stage. Fig. 9(a) shows that the system with lower code rate has better performance, because lower code rate indicates more significant error correction capacity with larger redundancy when the frame length is fixed. We also compare different error correction codes under the same code rate, i.e., RS, CC, and a concatenation of them, namely RS + CC under the same code rate. Fig. 9(b) shows that the system with the concatenated code performs better because its BER reaches the value below  $10^{-4}$  at the smaller SNR compared to the other counterparts.

V. CONCLUSIONS

This paper presented a novel approach for indoor provisioning of mobile services via low-voltage residential power lines, and investigated the feasibility of taking a power line communication (PLC) channel as the last hop of the C-RAN front-haul, where reliable transfer of the CPRI HFs is achieved via the PLC channel between the RU and DU. Particularly, we introduced CPG as an agent for creating a virtual CPRI link over a PLC channel to achieve the system capacity required by CPRI. Simulations showed that the CPG operating the proposed impulsive noise detection (IND) technique along with hybrid ARQ (HARQ) based re-transmission can effectively create a valid CPRI link over the noisy PLC channel without modification of any existing protocol operation and hardware arrangement (DU & RU). Specifically, we found that with low code rates in HARQ can yield a significant boost to the BER performance at a very limited expense in terms of higher redundancy.

REFERENCES

- [1] “Cisco Visual Networking Index: Forecast and Methodology 2017-2022,” February 2019.
- [2] F. Boccardi, R. W. Heath, A. Lozano, T. L. Marzetta, and P. Popovski, “Five disruptive technology directions for 5g,” *IEEE Communications Magazine*, vol. 52, no. 2, pp. 74–80, 2014.
- [3] Huawei, “5G Oriented Indoor Digitalization Solution White Paper,” 2017.
- [4] M. Hassan, S. H. R. Naqvi, and P.-H. Ho, “On CPRI based Front-hauling over Residential Power Lines,” in *2020 International Conference on Networking and Network Applications (NaNA)*, December 2020.
- [5] L. T. Berger, A. Schwager, and J. J. Escudero-Garzás, “Power line communications for smart grid applications,” *Journal of Electrical and Computer Engineering*, vol. 2013, pp. 1–16, 2013.
- [6] A. Mathur, M. R. Bhatnagar, and B. K. Panigrahi, “Performance evaluation of PLC with log-normal channel gain over Nakagami-m additive background noise,” in *2015 IEEE 26th Annual International Symposium on Personal, Indoor, and Mobile Radio Communications (PIMRC)*, pp. 824–829, 2015.
- [7] B. Tan and J. Tompson, “Powerline Communications Channel Modelling Methodology Based on Statistical Features,” *IEEE Power Delivery Transactions*, 03 2012.
- [8] S. Galli, “A simple two-tap statistical model for the power line channel,” in *2010 IEEE International Symposium on Power Line Communications and Its Applications (ISPLC)*, pp. 242–248, 2010.
- [9] L. D. Bert, P. Caldera, D. Schwingshackl, and A. M. Tonello, “On noise modeling for power line communications,” in *2011 IEEE International Symposium on Power Line Communications and Its Applications*, pp. 283–288, 2011.

- [10] H. Meng, Y. Guan, and S. Chen, "Modeling and analysis of noise effects on broadband power-line communications," *IEEE Transactions on Power Delivery*, vol. 20, no. 2, pp. 630–637, 2005.
- [11] A. Cortés, L. Díez, F. J. Cañete, and J. J. Sánchez-Martínez, "Analysis of the indoor broadband power-line noise scenario," *IEEE Transactions on Electromagnetic Compatibility*, vol. 52, no. 4, pp. 849–858, 2010.
- [12] S. Laksir, A. Chaoub, and A. Tamtaoui, "Impulsive noise reduction techniques in power line communication: A survey and recent trends," pp. 13–20, 2018.
- [13] K. M. Rabie and E. Alsusa, "Preprocessing based impulsive noise reduction for power-line communications," *IEEE Transactions on Power Delivery*, vol. 29, no. 4, pp. 1648–1658, 2014.
- [14] P. D. Mariyam, F. H. Juwono, P. D. Pamungkasari, and D. Gunawan, "How to deal with impulsive noise in ofdm-based plc: A survey," in *2017 International Conference on Electrical Engineering and Informatics (ICELTICs)*, pp. 163–168, 2017.
- [15] "Technical Report on Transport network support of IMT-2020/5G, v0." Telecommunication Standardization Sector of ITU, February 2019.
- [16] C. A. Duarte, "Self and Mutual Transmission Line Impedance Estimation by Means of the Non-Linear Least Squares Method," in *Simpósio Internacional sobre la Calidad de la Energía Eléctrica - SICEL*, vol. 7, 2013.
- [17] R. C. Silva, E. C. M. Costa, S. Kurokawa, and J. Pissolato, "Mutual coupling modeling in transmission lines directly in the phase domain," in *2011 IEEE Electrical Power and Energy Conference*, pp. 374–379, 2011.
- [18] H. Philipps, "Performance Measurements of Powerline Channels at High Frequencies," in *Proceedings of the 1998 International Symposium on Power-line Communications and Applications*, March 1998.
- [19] G. Prasad, L. Lampe, and S. Shekhar, "In-band full duplex broadband power line communications," *IEEE Transactions on Communications*, vol. 64, no. 9, pp. 3915–3931, 2016.
- [20] M. Zimmermann and K. Dostert, "Analysis and modeling of impulsive noise in broad-band powerline communications," *IEEE Transactions on Electromagnetic Compatibility*, vol. 44, no. 1, pp. 249–258, 2002.
- [21] "PLC Channel Characterization and Modelling." Seventh Framework Programme: Theme 3 ICT-213311 OMEGA, December 2008.
- [22] R. Hashmat, P. Pagani, A. Zeddani, and T. Chonave, "A channel model for multiple input multiple output in-home power line networks," in *2011 IEEE International Symposium on Power Line Communications and Its Applications*, pp. 35–41, 2011.
- [23] "Common Public Radio Interface (CPRI); Interface Specification." CPRI Specification V7.0 (2015–10-09), October 2015.
- [24] K. Khalil, P. Corlay, F. Coudoux, M. Gazalet, and M. Gharbi, "Analysis of the impact of impulsive noise parameters on BER performance of OFDM power-line communications," *CoRR*, vol. abs/1502.06821, 2015.
- [25] M. Zimmermann and K. Dostert, "A Multi-Path Signal Propagation Model for the Powerline Channel in the High Frequency Range," in *3rd International Symposium on Powerline Communications and its Applications*, (Lancaster, U.K.), p. 45–51, 1999.
- [26] R. Hashmat, P. Pagani, A. Zeddani, and T. Chonavel, "MIMO communications for inhome PLC networks: Measurements and results up to 100 MHz," in *2010 International Symposium on Power Line Communications and Its Applications*, pp. 120–124, 2010.
- [27] M. Lanoiselée and P. Siohan, "Analog front end design for gigabit power line communication," in *2012 IEEE International Symposium on Power Line Communications and Its Applications*, pp. 170–175, 2012.
- [28] L. T. Berger, A. Schwager, P. Pagani, and D. Schneider, *MIMO Power Line Communications: Narrow and Broadband Standards, EMC, and Advanced Processing*. USA: CRC Press, Inc., 2017.



**Mai Hassan** received her BS.c. and MS.c. degrees in Electronics and Communications Engineering from the American University in Cairo in 2008 and 2013 with highest honors. She has more than 9 years of experience in the industry in companies such as Intel Labs, Huawei Technologies and NSN in Egypt. She is currently pursuing her Ph.D. studies at the University of Waterloo, Canada. Her research interests include Network control systems, Radio access networks and Mobile radio networks.



**Limei Peng** received her Ph.D. degree from Jeonbuk National University in 2010. She is currently an Associate Professor with the School of Computer Science and Engineering, Kyungpook National University (KNU), Daegu, Republic of Korea. Her research interests include cloud computing, fog computing, data center networks, Internet of things (IoT)/Internet of vehicles (IoV), and 5G communications networks.



**Pin-Han Ho** received his Ph.D. degree from Queen's University in 2002. He is currently a Professor with the Department of Electrical and Computer Engineering, University of Waterloo, Canada. He has authored/co-authored over 350 refereed technical papers and several book chapters. His current research interests cover a wide range of topics in broadband wired & wireless communication networks.



**Haoran Mei** received his BS.c. and MS.c. degrees from Kyungpook National University (KNU) in Republic of Korea in 2018 and 2020. He is currently pursuing his Ph.D. studies at Kyungpook National University (KNU), Republic of Korea. His research interests include 5G communications networks.